ELSEVIER

Materials Chemistry and Physics 78 (2002) 464–473

MATERIALS CHEMISTRY AND PHYSICS

www.elsevier.com/locate/matchemphys

Phase transformations in a Cu–14.2Al–15.0Ni alloy

C.H. Chen*, T.F. Liu

Department of Materials Science and Engineering, National Chiao Tung University, Hsinchu, Taiwan 300, ROC

Received 21 May 2002; received in revised form 7 June 2002; accepted 14 June 2002

Abstract

In the as-quenched condition, the microstructure of the Cu–14.2Al–15.0Ni alloy was $D0_3$ phase containing extremely fine L–J precipitates. Since both fine $D0_3$ domains with $a/2\langle 1\,0\,0\rangle$ anti-phase boundaries (APBs) and small B2 domains with $a/4\langle 1\,1\,1\rangle$ APBs could be observed, the $D0_3$ phase existing in the as-quenched alloy should be formed by an A2 → B2 → $D0_3$ continuous ordering transition during quenching. It is worthwhile to note that the $a/4\langle 1\,1\,1\rangle$ APBs have never been observed by other workers in the Cu–Al–Ni ternary alloys before.

When the as-quenched alloy was aged at temperatures ranging from 400 to 1000 °C for longer times, the phase transformation sequence as the aging temperature increased was found to be (α + B2 precipitate) → (B2 + B2 precipitate) → B2 → A2. This transformation has also never been observed by other workers in the Cu–Al–Ni ternary alloys before.

Keywords: Cu–Al–Ni alloy; Phase transformation; Continuous ordering transition; Anti-phase boundaries; TEM

1. Introduction

Phase transformations in the Cu–Al–Ni ternary alloys have been studied by many workers [1–15]. On the basis of their studies, it is found that when an alloy with a chemical composition in the range of Cu–(12.8–15.1)Al–(3.0–7.7)Ni was solution heat-treated in the single β phase (A2, disordered body-centered cubic) region and then quenched into room temperature water or iced-brine rapidly, the microstructure was single $D0_3$ phase [1–4], or $D0_3$ phase containing extremely fine 2H-type precipitates [5–7]. After being aged at temperatures ranging from 325 to 550 °C for moderate times and then quenched, γ_2 particles started to occur within the $D0_3$ matrix at the aging temperature and the remaining $D0_3$ matrix would transform to γ_1' martensite during quenching [3,4,7]. When the as-quenched alloy was aged at this temperature range for longer times, fine B2 precipitates were observed to appear within the well-grown γ_2 particles and the remaining $D0_3$ matrix would completely transform to α phase (A1, disordered face-centered cubic) or a mixture of (α + β) phases at the aging temperature [7,9]. When the as-quenched alloy was aged in the range from 600 to 770 °C for longer times, the stable microstructure was found to be ($\beta + \gamma_2$) phases [7,9,10].

In the previous studies [1–14], it is clearly seen that although the phase transformations in the Cu–Al–Ni alloys have been extensively studied, most of the examinations were focused on the Cu–Al–Ni alloys with lower nickel content. Information concerning the microstructural development of the Cu–Al–Ni alloys with higher nickel content is very deficient. Therefore, the present investigation is an attempt to clarify the phase transformations in the Cu–14.2Al–15.0Ni alloy.

2. Experimental procedure

The alloy, Cu–14.2Al–15.0Ni, was prepared in a vacuum induction furnace by using 99.9% copper, 99.9% aluminum and 99.9% nickel. The melt was chill cast into a 30 mm × 50 mm × 200 mm copper mold. After being homogenized at 1000 °C for 72 h, the ingot was sectioned into 2.0 mm-thick slices. These slices were subsequently solution heat-treated at 1100 °C for 1 h and then quenched into room temperature water. The aging processes were performed at temperatures ranging from 400 to 1000 °C in a vacuum heat-treated furnace for various times and then quenched into room temperature water rapidly.

Electron microscopy specimens were prepared by means of a double-jet electropolisher with an electrolyte of 60% methanol and 40% nitric acid. The polishing temperature was kept in the range from −30 to −10 °C, and the current

* Corresponding author.
E-mail address: andychen.mse86g@nctu.edu.tw (C.H. Chen).

0254-0584/02/$ – see front matter © 2002 Elsevier Science B.V. All rights reserved.
PII: S0254-0584(02)00348-6

density was kept in the range from 2.0×10^4 to 4.0×10^4 A m^{-2}. Electron microscopy was performed on a JEOL JEM-2000FX scanning transmission electron microscope (STEM) operating at 200 kV. Elemental distributions were examined by using a LINK ISIS 300 energy-dispersive X-ray spectrometer (EDS). Quantitative analyses of elemental concentrations for Cu, Al and Ni were made with the aid of a Cliff–Lorimer ratio thin section method.

3. Results

Fig. 1(a) is a bright-field (BF) electron micrograph of the as-quenched alloy, indicating that a high density of extremely fine precipitates with a mottled structure was formed within the matrix. This feature is similar to that observed by other workers in the Cu–Al–Ni alloys [5,6]. Shown in Fig. 1(b)–(e) are four different selected-area diffraction patterns

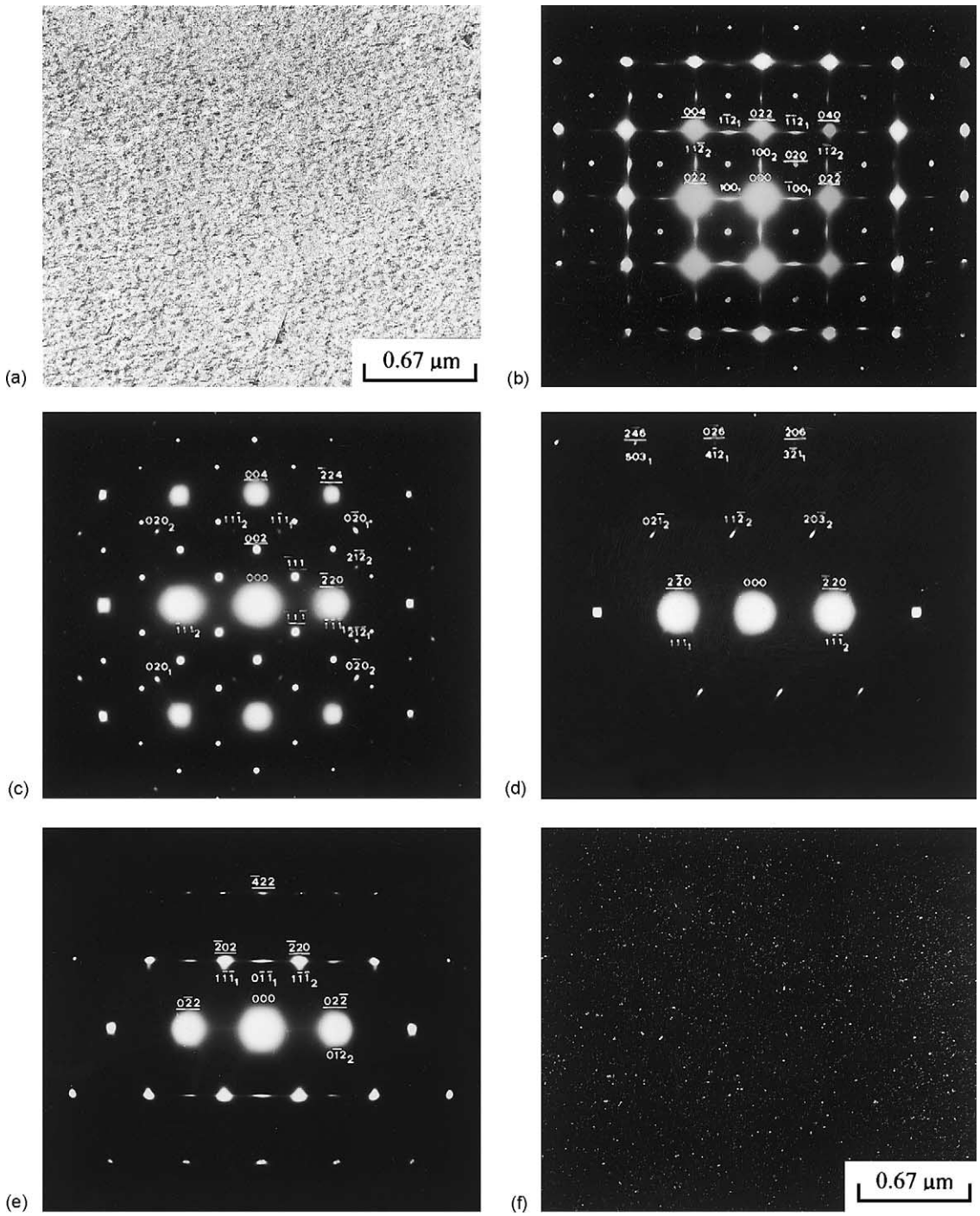

Fig. 1. Electron micrographs of the as-quenched alloy: (a) BF; (b)–(e) four SADPs. The zone axes of the $D0_3$ phase are (b) [1 0 0], (c) [1 1 0], (d) [3 3 1] and (e) [1 1 1], respectively ($\underline{h\,k\,l}$ = $D0_3$ phase, $h\,k\,l_{1or2}$ = L–J phase, 1: variant 1; 2: variant 2); (f) (0 2 0_1) L–J DF; (g) and (h) (0 0 2) and ($\bar{1}$ 1 1) $D0_3$ DF, respectively.

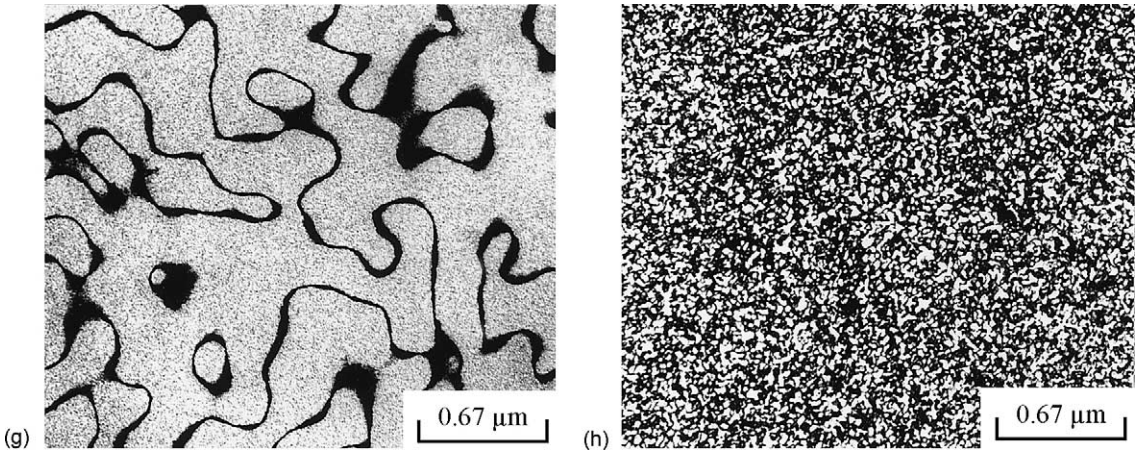

Fig. 1. (*Continued*).

(SADPs) of the as-quenched alloy. When compared with our previous studies in the Cu–14.6Al–4.3Ni and $Cu_{2.2}Mn_{0.8}Al$ alloys [15,16], it is found in these SADPs that the brighter and well-arranged reflection spots are of the ordered $D0_3$ phase, and the extra spots with streaks are derived from the L–J precipitates with two variants. Fig. 1(f) is a $(0\,2\,0_1)$ L–J dark-field (DF) electron micrograph, clearly revealing the presence of the extremely fine L–J precipitates. Accordingly, the microstructure of the as-quenched alloy was $D0_3$ phase containing extremely fine L–J precipitates. This is similar to that found by the present workers in the Cu–14.6Al–4.3Ni alloy [15]. Fig. 1(g), a $(0\,0\,2)$ $D0_3$ DF electron micrograph of the same area as Fig. 1(a), shows the presence of the small B2 domains with $a/4\langle 1\,1\,1\rangle$ anti-phase boundaries (APBs). Fig. 1(h) is a $(\bar{1}\,1\,1)$ $D0_3$ DF electron micrograph, indicating the presence of the extremely fine $D0_3$ domains with $a/2\langle 1\,0\,0\rangle$ APBs. In Fig. 1(g) and (h), it is also seen that the sizes of both B2 and $D0_3$ domains are very small. Therefore, it is confirmed that the $D0_3$ phase existing in the as-quenched alloy was formed by an A2 → B2 → $D0_3$ continuous ordering transition during quenching [17–21].

When the as-quenched alloy was aged at 400 °C for moderate times and then quenched, both the $D0_3$ and L–J phases disappeared and other two kinds of phases started to occur. A typical example is shown in Fig. 2(a). Fig. 2(b)–(d), three SADPs, indicate that the microstructure present in Fig. 2(a) is a mixture of B2 phase and γ_1' martensite with internal twins [3,13], and the orientation relationship between the B2 phase and the γ_1' martensite is $[0\,0\,1]_{B2}//[1\,0\,\bar{1}]_{\gamma_1'}$ and $(1\,\bar{1}\,0)_{B2}//(1\,2\,1)_{\gamma_1'}$. Fig. 2(e) and (f) show the $[1\,\bar{2}\,1]_{\gamma_1'}$ and $(1\,0\,0)$ B2 DF electron micrographs of the same area as Fig. 2(a), clearly revealing the presence of the γ_1' martensite and the extremely fine B2 precipitates, respectively. Transmission electron microscopy (TEM) examinations indicated that when the as-quenched alloy was aged at 400 °C for longer times, the size of the B2 precipitates increased with increasing the aging time and the remaining matrix had gradually decomposed into the disordered α phase, as illustrated in Fig. 3. Fig. 3(a) is a BF electron micrograph of the alloy aged at 400 °C for 24 h and then quenched. Fig. 3(b) and (c), two SADPs taken from an area covering the B2 precipitates and their surrounding α matrix, indicate that the orientation relationship between the B2 precipitate and the α matrix is $[1\,1\,\bar{1}]_{B2}//[1\,0\,\bar{1}]_{\alpha}$ and $(0\,1\,1)_{B2}//(1\,1\,1)_{\alpha}$, which corresponds to the Kurdjumov–Sachs (K–S) orientation relationship. Fig. 3(d) is a $(0\,0\,1)$ B2 DF electron micrograph, showing the presence of the well-grown B2 precipitates. It is thus concluded that the stable microstructure of the alloy at 400 °C should be a mixture of (α + B2 precipitate).

TEM observations of thin foils indicated that the mixture of (α + B2 precipitate) could be preserved up to 650 °C. A typical example is shown in Fig. 4(a), which is a BF electron micrograph of the alloy aged 650 °C for 24 h. Fig. 4(b), a $(0\,0\,1)$ B2 DF electron micrograph, reveals that the B2 precipitates were much larger than those observed in the alloy aged at 400 °C. Fig. 4(c) is an SADP taken from an area covering a B2 precipitate and its surrounding α matrix, indicating that the orientation relationship between the B2 precipitate and the α matrix is $[1\,1\,\bar{1}]_{B2}//[1\,0\,\bar{1}]_{\alpha}$ and $(0\,1\,1)_{B2}//(1\,1\,1)_{\alpha}$, which is also of the K–S orientation relationship.

Fig. 5(a) shows a BF electron micrograph of the alloy aged at 700 °C for 2 h and then quenched, revealing that the B2 precipitates could be observed within the matrix. Shown in Fig. 5(b) is an SADP taken from the matrix, indicating that the microstructure was the mixture of ($D0_3$ + L–J) phases. Fig. 5(c) and (d) are $(0\,2\,0_1)$ L–J and $(\bar{1}\,1\,1)$ $D0_3$ DF electron micrographs of the same area as Fig. 5(a), exhibiting the presence of the L–J precipitates and $D0_3$ domains, respectively. It is clear in Fig. 5(c) and (d) that the sizes of both the L–J precipitates and the $D0_3$ domains are very extremely fine. It is therefore reasonable to believe that these two phases were formed during quenching from the aging temperature; otherwise, their sizes should be increased at the aging temperature [17,21,22]. Fig. 5(e), a $(0\,0\,2)$ $D0_3$ DF

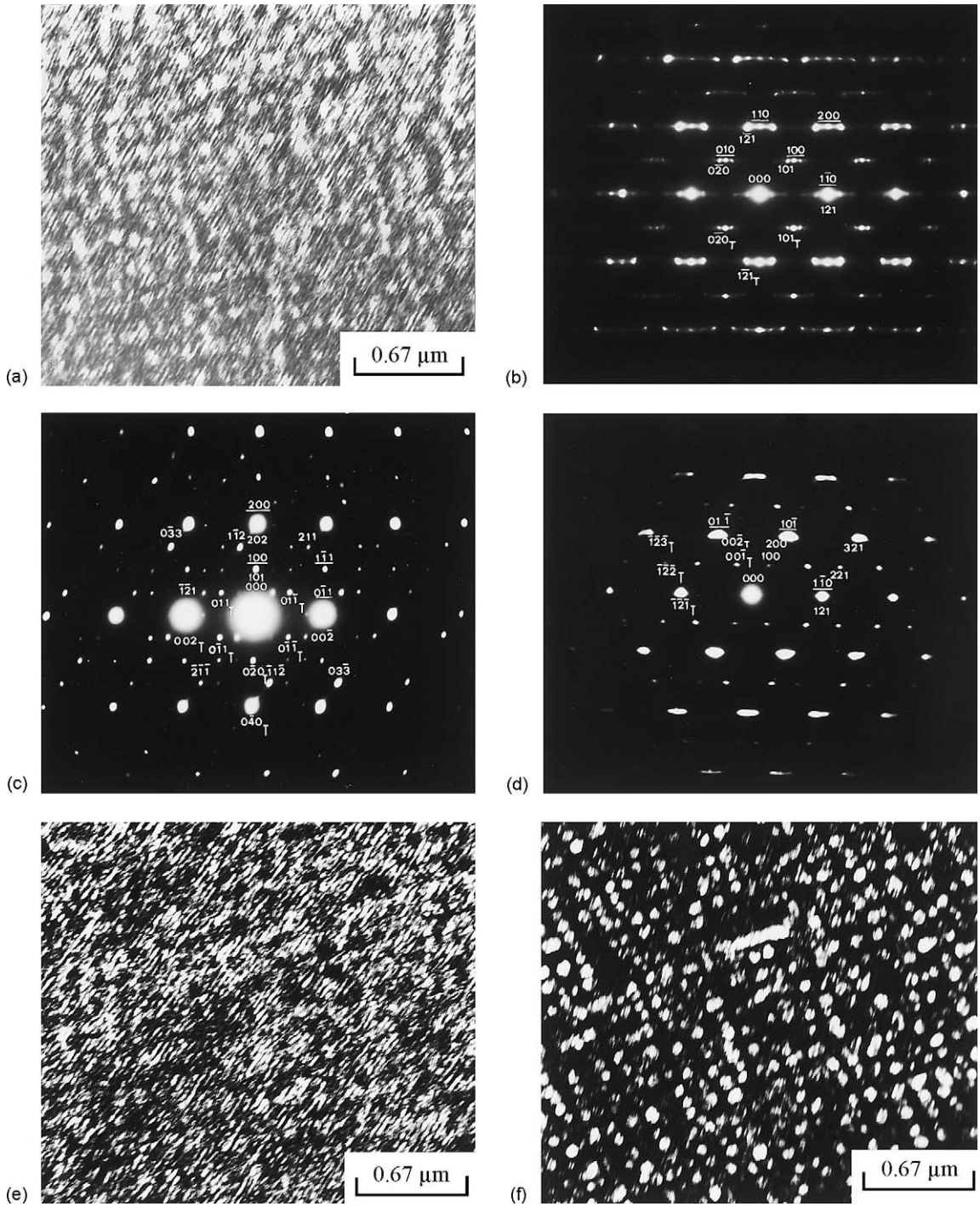

Fig. 2. Electron micrographs of the alloy aged at 400 °C for 10 min: (a) BF; (b)–(d) three SADPs. The zone axes of the B2 precipitate are (b) [0 0 1], (c) [0 1 1] and (d) [1 1 1], respectively ($\underline{h\,k\,l}$ = B2 precipitate, $h\,k\,l = \gamma_1'$ martensite, $h\,k\,l_T$ = internal twin); (e) and (f) $(1\,\bar{2}\,1)\gamma_1'$ and (1 0 0) B2 DF, respectively.

electron micrograph, shows that the B2 domains have grown to reach the whole grain and no evidence of the $a/4\langle 1\,1\,1\rangle$ APBs could be detected. This indicates that the microstructure of the matrix was the B2 phase. Apparently, the stable microstructure of the alloy present at 700 °C was the B2 phase containing B2 precipitates. It is worthwhile to note that the coexistence of two kinds of ordered B2 phase has not previously been observed by other workers in the Cu–Al–Ni alloys before.

Shown in Fig. 6(a) is a (0 0 2) $D0_3$ DF electron micrograph of the alloy aged at 750 °C for 1 h and then quenched. It reveals that along with the growth of the B2 domains, the $a/4\langle 1\,1\,1\rangle$ APBs had gradually disappeared. Fig. 6(b) and (c) $(\bar{1}\,1\,1)$ $D0_3$ and $(0\,2\,0_1)$ L–J DF electron micrographs of

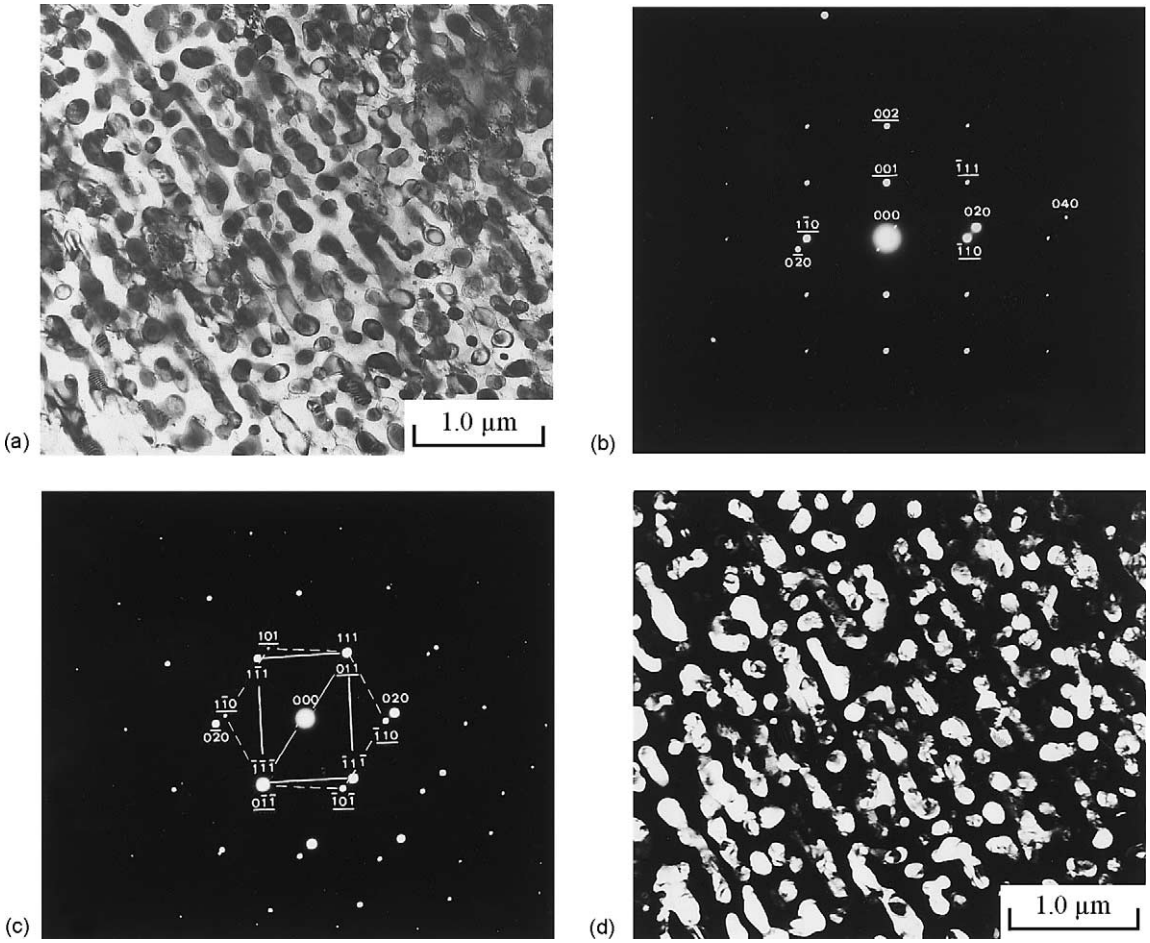

Fig. 3. Electron micrographs of the alloy aged at 400 °C for 24 h: (a) BF; (b) and (c) two SADPs, taken from an area covering the B2 precipitates and their surrounding a matrix. The zone axes of the B2 precipitate are (b) [1 1 0] and (c) [1 1 $\bar{1}$], respectively ($\underline{h\,k\,l}$ = B2 precipitate, $h\,k\,l$ = α phase); (d) (0 0 1) B2 DF.

the same area as Fig. 6(a), show that only quenched-in $D0_3$ domains and L–J precipitates (the sizes being comparable to those observed in the as-quenched alloy) could be observed. This indicates that the microstructure of the alloy present at 750 °C was the single B2 phase.

Progressively higher temperature aging and quenching experiments indicated that the single B2 phase was preserved up to 975 °C. An example is shown in Fig. 7(a). However, in an alloy aged at 1000 °C for 1 h and then quenched, only quenched-in B2 domains could be detected, as illustrated in Fig. 7(b). This indicates that the microstructure existing at 1000 °C or above was a single disordered β phase.

4. Discussion

The presence of the $a/4\langle 1\,1\,1\rangle$ APBs is a remarkable feature in the present study. In the previous studies of the Cu–(12.8–15.1)Al–(3.0–7.7)Ni alloys [1–15], it is clear that in the as-quenched condition, no $a/4\langle 1\,1\,1\rangle$ APBs could be observed. For the absence of the $a/4\langle 1\,1\,1\rangle$ APBs, several workers proposed that although the $D0_3$ phase was formed by an A2 → B2 → $D0_3$ transition during quenching from the single β (A2) phase region, the $a/4\langle 1\,1\,1\rangle$ APB energy in the Cu–Al–Ni and Cu–Al–Mn alloys was very high, which would lead the B2 domains to grow up to the whole grains during quenching [4,23,24]. Therefore, no $a/4\langle 1\,1\,1\rangle$ APBs could be observed. In contrast to the above proposition, other workers claimed that the $D0_3$ phase was occurred–an A2 → $D0_3$ transition, rather than the A2 → B2 → $D0_3$ transition [1,3,7]. The A2 → B2 transition produced $a/4\langle 1\,1\,1\rangle$ APBs and the B2 → $D0_3$ transition produced $a/2\langle 1\,0\,0\rangle$ APBs [17,18]. Therefore, no $a/4\langle 1\,1\,1\rangle$ APBs were formed. In the present study, it is obvious that the $a/4\langle 1\,1\,1\rangle$ APBs indeed could be detected. This result strongly confirms that the $D0_3$ phase existing in the as-quenched alloy should be formed through an A2 → B2 → $D0_3$ transition during quenching. Furthermore, in addition to contain higher nickel content, the chemical composition of the present alloy is similar to that investigated by other workers in the Cu–Al–Ni alloys [1–11]. It seems to imply that the increase of the nickel

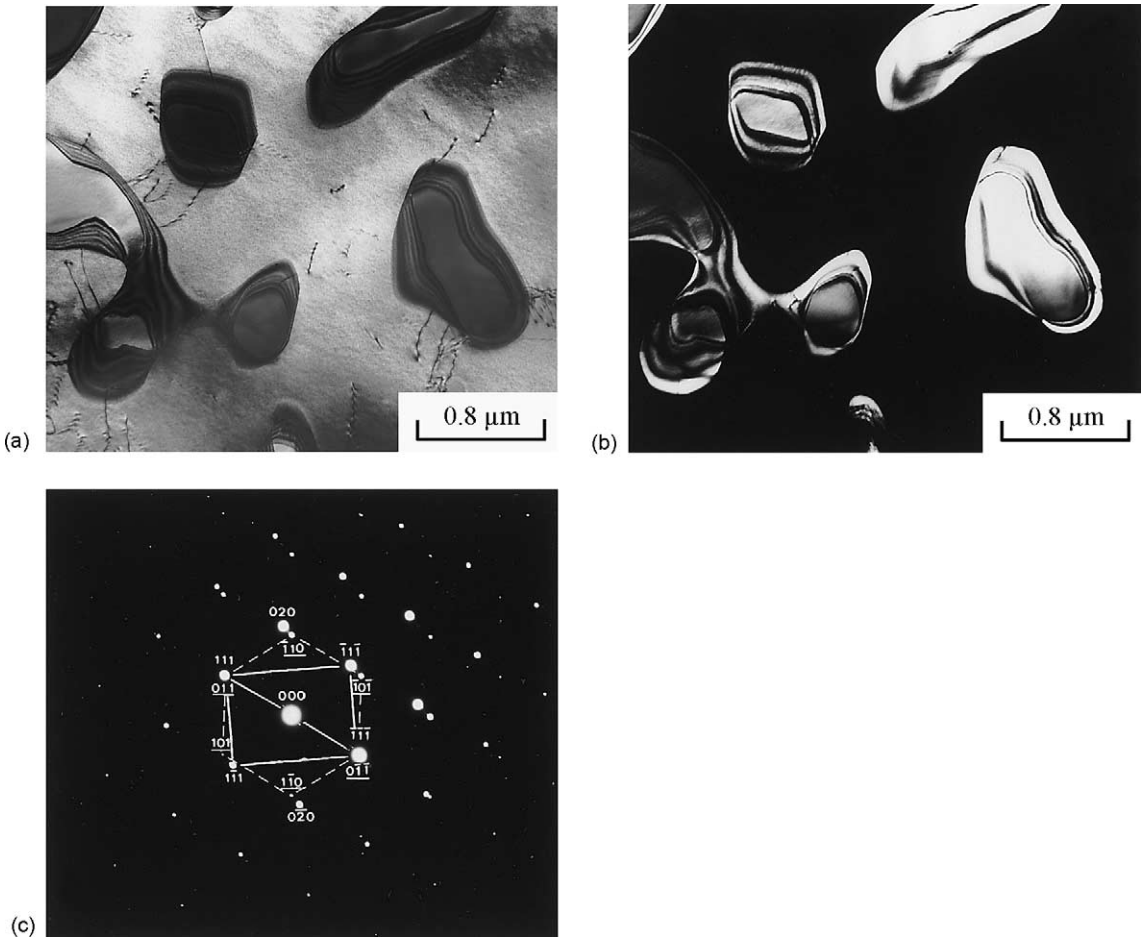

Fig. 4. Electron micrographs of the alloy aged at 650 °C for 24 h: (a) BF; (b) (0 0 1) B2 DF; (c) an SADP taken from an area covering the B2 precipitate and its surrounding α matrix. The zone axes of the B2 precipitate and α phase are [1 1 1̄] and [1 0 1̄], respectively ($\underline{h\,k\,l}$ = B2 precipitate, $h\,k\,l$ = α phase).

content could decrease the $a/4\langle 1\,1\,1\rangle$ APB energy; therefore, the $a/4\langle 1\,1\,1\rangle$ APBs became visible.

In the as-quenched condition, the microstructure of the present alloy was $D0_3$ phase containing extremely fine L–J precipitates and no γ_1' martensite could be observed. This indicates that in the alloy with the chemical composition of Cu–14.2Al–15.0Ni, the $D0_3 \rightarrow \gamma_1'$ martensitic transformation temperature should be below room temperature. However, when the present alloy was aged at 400 °C for moderate times and then quenched, the microstructure was the mixture of (γ_1'+B2 precipitate). This feature has never been observed by other workers in the Cu–Al–Ni alloys before. In order to clarify this feature, an STEM–EDS study was performed. Fig. 8(a)–(c) represent three typical EDS spectra taken from the as-quenched alloy and a B2 precipitate as well as the γ_1' martensite in the alloy aged at 400 °C for 10 min, respectively. The average weight percentages of alloying elements examined by analyzing at least 10 different EDS spectra of each phase are listed in Table 1. For comparison, the chemical compositions of the B2 and α phases existing in the alloy aged at 400 °C for 24 h are also listed in Table 1. It is noted here that since in the present study the EDS analyses were

Table 1
Chemical compositions of the phases revealed by EDS

Heat treatment	Phase	Chemical composition (wt.%)		
		Cu	Al	Ni
As-quenched	$D0_3$ + L–J	70.77 ± 0.72	14.19 ± 0.35	15.04 ± 0.48
400 °C for 10 min	B2 precipitate	56.06 ± 1.56	18.67 ± 1.05	25.27 ± 1.11
	γ_1' Martensite (remaining $D0_3$ phase)	83.71 ± 1.02	9.82 ± 0.98	6.47 ± 1.05
400 °C for 24 h	B2 precipitate	12.29 ± 0.67	25.91 ± 0.51	61.80 ± 0.56
	α Phase	91.71 ± 1.02	6.40 ± 0.36	1.89 ± 0.32

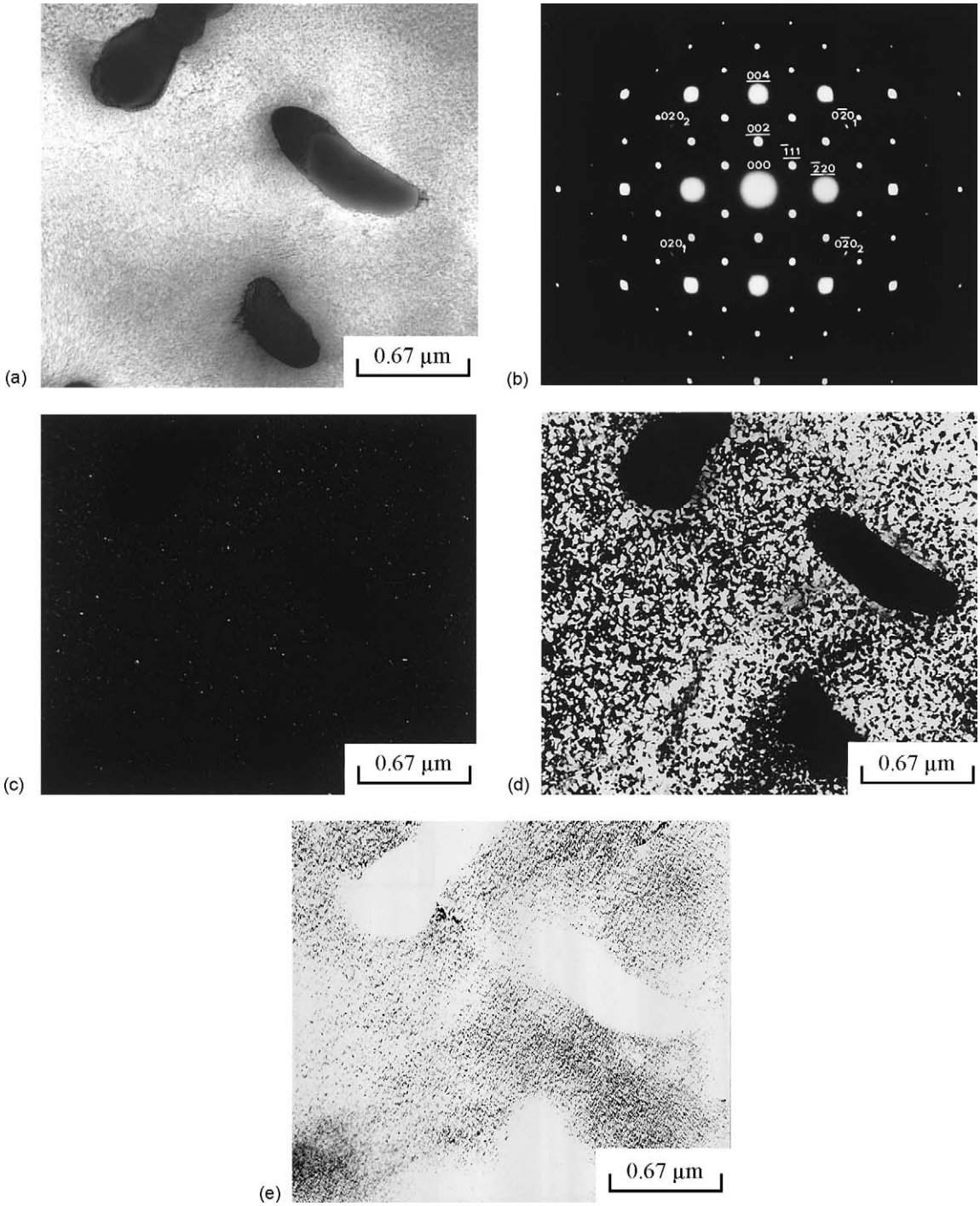

Fig. 5. Electron micrographs of the alloy aged at 700 °C for 2 h: (a) BF; (b) an SADP taken from the matrix. The zone axis of the $D0_3$ phase is [1 1 0] ($\underline{h\,k\,l}$ = $D0_3$ phase, $h\,k\,l_{1or2}$ = L–J phase, 1: variant 1; 2: variant 2); (c) $(0\,2\,0_1)$ L–J DF; (d) and (e) $(\bar{1}\,1\,1)$ and $(0\,0\,2)$ $D0_3$ DF, respectively.

made in the STEM mode on thin films (not on the extracted phase) and the size of the B2 precipitates (about 60 nm) examined is slightly larger than that of the electron beam spot (40 nm) produced on the JEOL JEM-2000FX STEM, some errors in the exact percentage of elemental concentrations in the B2 precipitates are inevitable. However, it is seen in Fig. 8 and Table 1 that both the nickel and aluminum concentrations in the B2 precipitates are much greater than those in the as-quenched alloy, γ_1' martensite or α phase. Therefore, these analyses are still enough to permit an inference that the B2 precipitates are enriched in both nickel and aluminum. On the basis of the above analyses, it is clear that when the as-quenched alloy was aged at 400 °C for moderate times, a high density of the B2 precipitates started to appear. Since the nickel and aluminum concentrations in the B2 precipitates are very high, the remaining matrix would be

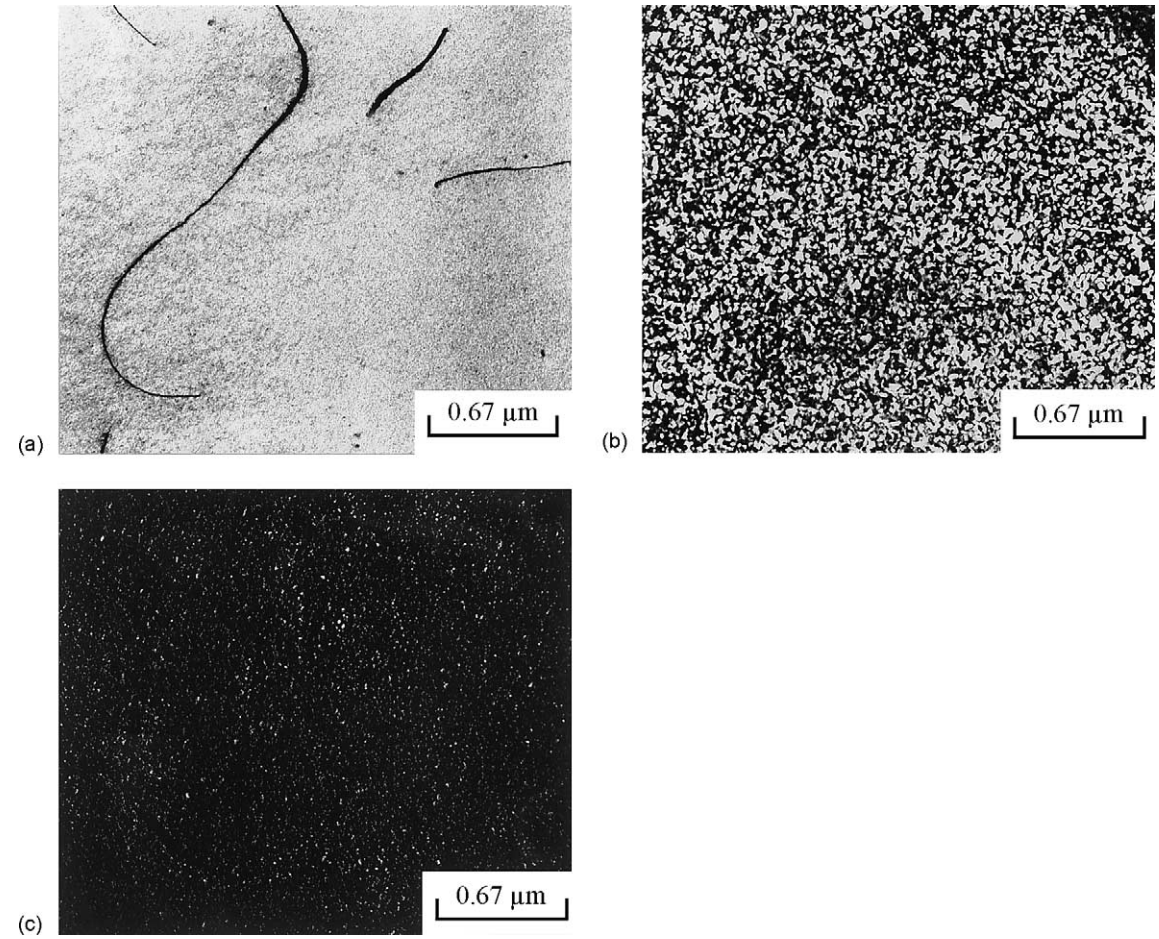

Fig. 6. Electron micrographs of the alloy aged at 750 °C for 1 h: (a) and (b) (0 0 2) and ($\bar{1}$ 1 1) $D0_3$ DF, respectively; (c) (0 2 0_1) L–J DF.

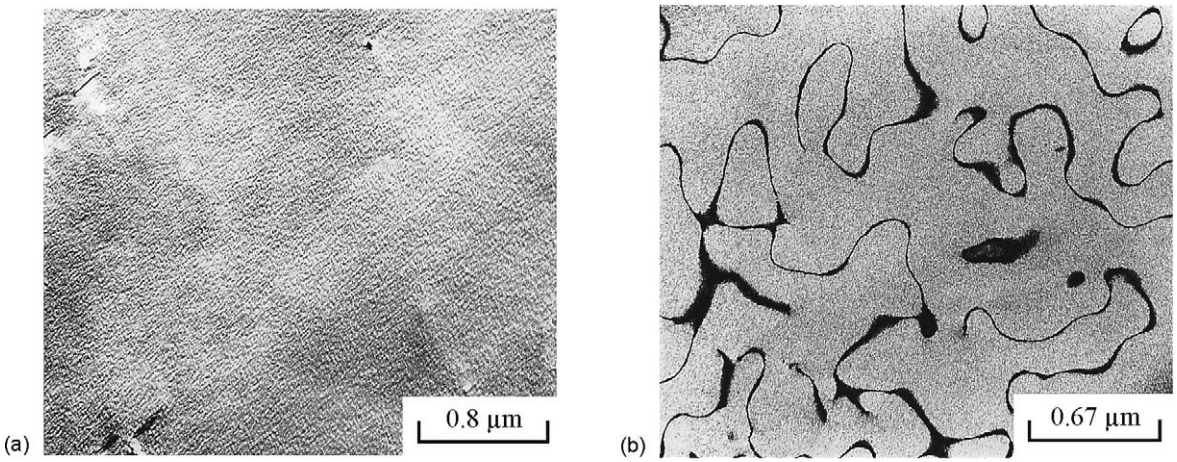

Fig. 7. (0 0 2) $D0_3$ DF electron micrographs of the alloy aged at (a) 975 °C for 1 h and (b) 1000 °C for 1 h, respectively.

lowered in both nickel and aluminum. The lower concentrations of both nickel and aluminum would cause the martensitic transformation temperature of the remaining matrix to be higher [2,7,11], which induced the $D0_3 \rightarrow \gamma_1'$ martensitic transformation that would occur during quenching from the aging temperature. This result is consistent with the observation in Fig. 2. Furthermore, with increasing the aging time at 400 °C, the B2 precipitates would grow. Along with the growth of the B2 precipitates, the remaining matrix would be depleted in both nickel and aluminum. The insufficient

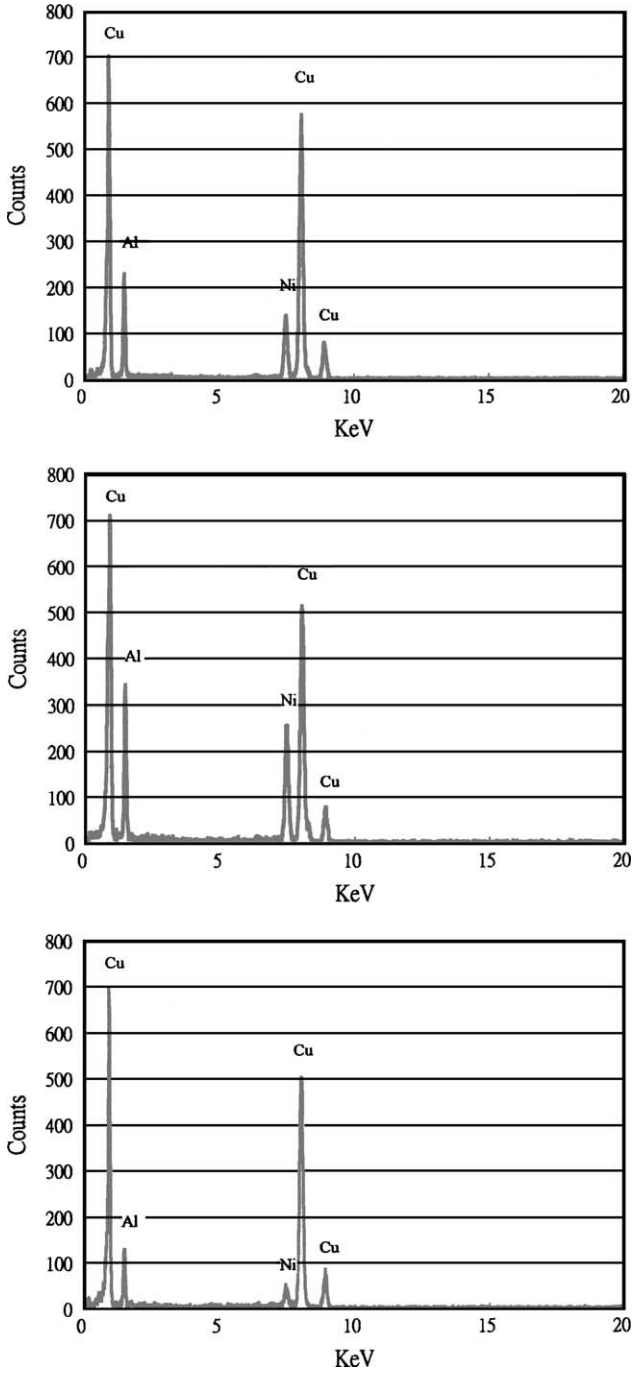

Fig. 8. Three typical EDS spectra obtained from (a) as-quenched alloy, (b) a B2 precipitate as well as (c) γ_1' martensite in the alloy aged at 400 °C for 10 min.

concentration of aluminum would cause the $D0_3$ matrix to become unstable [7,25]. Consequently, the remaining $D0_3$ matrix would transform to the Cu-rich α phase, which is consistent with the observation in Fig. 3.

Finally, two more features are worthwhile to note as follows: (1) the γ_2 precipitates were always reported to be observed in the Cu–(12.8–15.1)Al–(3.0–7.7)Ni alloys after being aged at temperatures ranging from 200 to 770 °C for various times [1–15]. However, in the present study, no evidence of the γ_2 precipitates could be detected. This result implies that the higher nickel addition in the Cu–Al–Ni alloy would unfavor the precipitation of the γ_2 phase. (2) In the previous studies of the Cu–Al–Ni ternary alloys [1–15], no information concerning the A2 → B2 transition temperature has been provided in the literatures. However, according to the phase diagram of the Cu–Al binary alloys [25,26], it is seen that the A2 → B2 transition temperature of a Cu–14.2–Al alloy was about 710 °C. In the present alloy, this transition temperature was found to be raised to somewhere between 975 and 1000 °C. This indicates that the nickel addition in the Cu–Al binary alloys would expand the B2 phase field.

5. Conclusions

The phase transformations in the Cu–14.2Al–15.0Ni alloy have been investigated by using TEM.

(1) In the as-quenched condition, the microstructure was $D0_3$ phase containing extremely fine L–J precipitates. The $D0_3$ phase was formed by an A2 → B2 → $D0_3$ continuous ordering transition during quenching.
(2) When the as-quenched alloy was aged at 400 °C for moderate times and then quenched, the microstructure was the mixture of (γ_1' + B2 precipitate). This feature has never been observed by other workers in the Cu–Al–Ni alloys before.
(3) When the as-quenched alloy was aged at temperatures ranging from 400 to 1000 °C for longer times, the phase transformation sequence as the temperature increased was found to be (α + B2 precipitate) → (B2 + B2 precipitate) → B2 → A2.
(4) The higher nickel addition in the Cu–Al–Ni alloy would unfavor the precipitation of the γ_2 phase.
(5) The nickel addition in the Cu–Al binary alloys would expand the B2 phase field.

Acknowledgements

The author is pleased to acknowledge the financial support of this research by the National Science Council, Republic of China under Grant NSC90-2216-E-009-044. He is also grateful to M.H. Lin for typing.

References

[1] M.A. Dvorack, N. Kuwano, S. Polat, H. Chen, C.M. Wayman, Scripta Metall. 17 (1983) 1333–1336.
[2] N.F. Kennon, D.P. Dunne, L. Middleton, Metall. Trans. A 13 (1982) 551–555.
[3] N. Kuwano, C.M. Wayman, Metall. Trans. A 15 (1984) 621–626.
[4] N. Zárubová, A. Gemperle, V. Novák, Mater. Sci. Eng. A 222 (1997) 166–174.

[5] K. Otsuka, H. Sakamoto, K. Shimizu, Trans. JIM 20 (1979) 244–254.
[6] K. Otsuka, H. Kubo, C.M. Wayman, Metall. Trans. A 12 (1981) 595–605.
[7] J. Singh, H. Chen, C.M. Wayman, Metall. Trans. A 17 (1986) 65–72.
[8] J. Singh, H. Chen, C.M. Wayman, Scripta Metall. 19 (1985) 887–890.
[9] J. Singh, H. Chen, C.M. Wayman, Scripta Metall. 19 (1985) 231–234.
[10] D.P. Dunne, N.F. Kennon, Met. Forum 4 (3) (1981) 176–183.
[11] V. Agafonov, P. Naudot, A. Dubertret, B. Dubois, Scripta Metall. 22 (1988) 489–494.
[12] Y.S. Sun, G.W. Lorimer, N. Ridley, Metall. Trans. A 21 (1990) 575–588.
[13] T. Hara, T. Ohba, S. Miyazaki, K. Otsuka, Mater. Trans. JIM 33 (12) (1992) 1105–1113.
[14] D. Hull, R.D. Garwood, J. Insti. Metals 86 (1957–58) 485–492.
[15] J. Tan, T.F. Liu, Mater. Chem. Phys. 70 (2001) 49–53.
[16] S.C. Jeng, T.F. Liu, Metall. Trans. A 26 (1995) 1353–1365.
[17] P.R. Swann, W.R. Duff, R.M. Fisher, Metall. Trans. 3 (1972) 409–419.
[18] S.M. Allen, J.W. Cahn, Acta Metall. 24 (1976) 425–437.
[19] J.W. Lee, T.F. Liu, Mater. Chem. Phys. 69 (2001) 192–198.
[20] C.C. Wu, J.S. Chou, T.F. Liu, Metall. Trans. A 22 (1991) 2265–2276.
[21] T.F. Liu, J.S. Chou, C.C. Wu, Metall. Trans. A 21 (1990) 1891–1899.
[22] T.F. Liu, S.C. Jeng, C.C. Wu, Metall. Trans. A 23 (1992) 1395–1401.
[23] Y.G. Nesterenko, I.A. Osipenko, S.A. Firstov, Fiz. Met. Metalloved. 27 (1) (1969) 135–140.
[24] M. Bouchard, G. Thomas, Acta Metall. 23 (1975) 1485–1500.
[25] X.J. Liu, I. Ohnuma, R. Kainuma, K. Ishida, J. Alloys Comp. 264 (1998) 201–208.
[26] R. Kainuma, N. Satoh, X.J. Liu, I. Ohnuma, K. Ishida, J. Alloys Comp. 266 (1998) 191–200.